Time Domain Sensitivity of the Tracking Error

S. O'Neil, *Member, IEEE*, S. G. Schirmer, *Member, IEEE*, F. C. Langbein, *Member, IEEE*, C. A. Weidner, and E. Jonckheere, *Life Fellow, IEEE*

***Abstract*— A strictly time-domain formulation of the log-sensitivity of the error signal to structured plant uncertainty is presented and analyzed through simple classical and quantum systems. Results demonstrate that across a wide range of physical systems, maximization of performance (minimization of the error signal) asymptotically or at a specific time comes at the cost of increased log-sensitivity, implying a time-domain constraint analogous to the frequency-domain identity $\mathbf{S(s)+T(s)=I}$. While of limited value in classical problems based on asymptotic stabilization or tracking, such a time-domain formulation is valuable in assessing the reduced robustness cost concomitant with high-fidelity quantum control schemes predicated on time-based performance measures.**

I. Introduction

Traditionally, within the realm of feedback control, sensitivity analysis of a closed-loop system to uncertain parameters is accomplished in the frequency domain. Standard definitions for the sensitivity examine the derivative of the closed-loop plant $T(s)$ to differential perturbations in a given element $K(s)$ and are given by $\partial T(s)/\partial K(s)$. As this measurement scales with the units used to describe the plant and parameter, a more useful formulation is given as the *log-sensitivity* of the closed-loop plant to variations in a given element through [1]

$$\frac{\partial T(s)/T(s)}{\partial K(s)/K(s)} = \frac{\partial T(s)}{\partial K(s)}\frac{K(s)}{T(s)}. \tag{1}$$

While valuable from a frequency-domain perspective, this method does not yield information about how the log-sensitivity evolves with time, time-domain considerations often being grouped into performance measures such as rise and settling times.

Some researchers have proposed methods for analyzing sensitivity of system performance in the time domain, though the methods tend to be system-specific. In [2] and [3], methods for analyzing the sensitivity of the output transient response for distributed transmission lines and microwave circuits are proposed. Additionally, [4] and [5] provide methods for computing time-domain sensitivity measures for active and passive circuits. In particular, [5] convincingly demonstrates the computational efficiency of analytic methods to brute-force comprehensive perturbation analysis. While providing valuable methods for computing sensitivity in the time-domain, the current research in this area does not provide a predictive model for how sensitivity behaves in relation to performance metrics. This requirement for a predictive, time-domain model to gauge trade-offs in robustness and performance of a given control scheme is becoming increasingly important in the field of quantum technology. Control problems in this field ranging from fast state transfer to the implementation of quantum gates are fundamentally time-based and not well-described by existing frequency-domain methods [6], [7], [8]. Furthermore, the eigenstructure of quantum systems presents poles at the origin or on the imaginary axis that preclude use of the more common small-gain theorem-based robustness analysis methods such as structured singular value analysis [9], [10].

In this paper, we extend the concept of the log-sensitivity from the frequency-domain analysis of transfer functions to the time-domain analysis of a signal. In particular, we examine the error signal $e(t) = y(t) - r(t)$ of a SISO system to structured uncertainty in the system parameters. We first demonstrate the methodology with a pair of classical systems and then extend the concept to quantum systems where time-domain specifications, particularly read-out time (i.e., the time at which the state of the system is measured), are crucial to system performance [11], [12], [13]. The main contribution of this paper is to provide a characterization of how the log-sensitivity of the error behaves as the output approaches the desired reference input. We show that the log-sensitivity of the error diverges to infinity as $y(t) \to r(t)$. Furthermore, the manner in which the log-sensitivity diverges is characterized by the dominant eigenvalue(s) of the closed-loop system and structure of the uncertain system parameters.

In Section II, we establish the basic paradigm to calculate the log-sensitivity of the error in terms of a classical Single-Input, Single-Output (SISO) system with full-state feedback. Here the pole-placement simultaneously meets design specifications and provides zero-steady state error as in [14]. In Section III, we provide the derivation of the time-domain log-sensitivity of the error, prove that the limit of the log-sensitivity diverges as the output approaches the desired steady-state value, and characterize this divergence in terms of the dominant eigenvalue(s) of the closed-loop system. In Sections IV, V, VI, and VII we apply our analysis to a pair of classical feedback systems and a pair of quantum systems, one subject to dissipation and one that evolves unitarily; this

This research was supported in part by NSF Grant IRES-1829078.

SON and EAJ are with the Department of Electrical and Computer Engineering, University of Southern California, Los Angeles, CA 90089 USA (email: seanonei@usc.edu, jonckhee@usc.edu).

SGS is with the Faculty of Science & Engineering, Swansea University, Swansea SA2 8PP, UK (e-mail: s.m.shermer@gmail.com).

FCL is with the School of Computer Science and Informatics, Cardiff University, Cardiff CF24 4AG, UK (e-mail: frank@langbein.org).

CAW is with the Quantum Engineering Technology Laboratories, H. H. Wills Physics Laboratory and Department of Electrical and Electronic Engineering, University of Bristol, Bristol BS8 1FD, United Kingdom (e-mail: c.weidner@bristol.ac.uk).

latter case is particularly interesting due to the difficulty of applying classical robust control methods to these systems, except in some special cases [15], [16], [17].

II. Preliminaries

We consider the general-case of a SISO system with multiple states and the control objective of tracking a step input with zero error. The system is represented by

$$\begin{aligned} \dot{x} &= \tilde{A}x + bu, \\ y &= cx. \end{aligned} \tag{2}$$

Here, $c \in \mathbb{R}^{1\times N}$ and $b \in \mathbb{R}^{N\times 1}$ since we consider a SISO system. The matrix $\tilde{A} \in \mathbb{R}^{N\times N}$ is given by $\tilde{A} = A_0 + S\xi_0 + S(\xi - \xi_0)$. The nominal dynamics matrix is $A_0 + S\xi_0$ and $\xi \in [\xi_1, \xi_2]$ is an uncertain parameter with nominal value $\xi_0 \in [\xi_1, \xi_2]$. This uncertain parameter enters the dynamics additively through the matrix S.

Assuming the system is controllable, we use state feedback to place the poles of the system in the open left-half plane. Introducing the reference signal $r(t)$, the system input is $u(t) = kx(t) + k_0 r(t)$ where $k \in \mathbb{R}^{1\times N}$ is the vector of static feedback gains and k_0 is the scalar gain used to scale the reference. Including the state feedback, we have the state matrix $A = \tilde{A} - bk = A_0 - bk + S\xi$ and the state equation becomes

$$\dot{x} = Ax + bk_0 r(t) \tag{3}$$

where $r(t)$ is a step function.

We determine the time-domain state evolution as

$$\begin{aligned} x(t) &= e^{At}x(0) + \int_0^t e^{A(t-\tau)} bk_0 r(\tau)\, d\tau \\ &= e^{At}x(0) + k_0 r_0 e^{At} \int_0^t e^{-A\tau} b\, d\tau, \end{aligned} \tag{4}$$

where r_0 is the magnitude of the step input $r(t)$ which will be taken as unity. Without loss of generality and to simplify the exposition, we set $x(0) = 0$ and constrain our analysis to the zero-state response so that

$$x(t) = k_0(e^{tA} - I)A^{-1}b. \tag{5}$$

The term $-A^{-1}b$ enters as the vector of steady-state values of the step input-to-state response of the transfer function $(sI - A)^{-1}b = G(s)$. This follows immediately from evaluation of $G(s)|_{s=0} = -A^{-1}b$.

Since our goal is to track a unity step input so that $y(t) = cx(t) = r(t) = 1$, we ultimately want $-k_0 cA^{-1}b = r_0 = 1$ or $k_0 = -(cA^{-1}b)^{-1}$. For simplicity, we write $A^{-1}b$ as the vector β. The output becomes

$$y(t) = cx(t) = k_0 ce^{At}\beta - k_0 c\beta = k_0 ce^{At}\beta + 1, \tag{6}$$

and we define the error signal as

$$e(t) = r(t) - y(t) = -k_0 ce^{At}\beta. \tag{7}$$

III. Log Sensitivity of the Error

With the time-domain error signal in (7), we compute the log-sensitivity of the error to differential perturbations in the parameter ξ. We define the log-sensitivity of the error as

$$s(\xi_0, t) = \frac{\partial e(t)}{\partial \xi} \frac{\xi}{e(t)}\bigg|_{\xi=\xi_0}. \tag{8}$$

In general, the matrices $A = A_0 - bk + S\xi$ and S do not commute. As such, calculation of the derivative of $e(t)$ with respect to the uncertain parameter ξ follows from [18] where

$$\begin{aligned} \frac{\partial e(t)}{\partial \xi} &= -k_0 c \frac{\partial}{\partial \xi} e^{(A_0 - bk + S\xi)t}\beta \\ &= -k_0 c \left(\int_0^t e^{(t-\tau)A} S e^{\tau A} d\tau \right) \beta. \end{aligned} \tag{9}$$

To be absolutely precise, note that in the limit as $\Delta\xi \to 0$, we define the directional derivative of e^{At} in the direction of S as in [18]

$$\begin{aligned} D_S(t, A) &= \lim_{\Delta\xi\to 0} \frac{1}{\Delta\xi}(e^{t(A_0 - bk + S(\xi_0 + \Delta\xi))} - e^{t(A_o - bk + S\xi_0)}) \\ &= \lim_{\Delta\xi\to 0} \frac{1}{\Delta\xi}(e^{t(A + S\Delta\xi)} - e^{tA}), \end{aligned} \tag{10}$$

where $\Delta\xi = \xi - \xi_0$. Hence, $S\xi_0$ is included in $A = A_0 - bk + S\xi_0$ throughout the derivative, and we consider only differential perturbations of $\Delta\xi$ from ξ_0 in the direction of the structure matrix S.

We assume that A is diagonalizable so that $A = M\Lambda M^{-1}$ and $e^{At} = Me^{t\Lambda}M^{-1}$. We then have, from [18],

$$\frac{\partial}{\partial \xi} e^{tA} = M(\bar{S} \odot \Phi(t))M^{-1}, \tag{11}$$

where $\bar{S} = M^{-1}SM$, $\odot$ is the Hadamard product, and the elements of $\Phi(t)$ are defined as

$$\phi_{k,l}(t) = \phi_{l,k}(t) = \begin{cases} \frac{e^{\lambda_k t} - e^{\lambda_l t}}{\lambda_k - \lambda_l} & \text{for } k \neq l, \\ te^{\lambda_k t} & \text{for } k = l, \end{cases} \tag{12}$$

where λ_k are the eigenvalues of $A = A_0 - bk + S\xi_0$. Furthermore, we separate this into two matrices so that $(\bar{S} \odot \Phi(t)) = (X_D(t) + X_N(t))$. Here, $X_D(t)$ is a diagonal matrix of the form $\mathbf{diag}(t\bar{s}_{kk}e^{\lambda_k t})$. $X_N(t)$ consists of off-diagonal elements of the form

$$\bar{s}_{kl} \frac{e^{\lambda_k t} - e^{\lambda_l t}}{\lambda_k - \lambda_l} \tag{13}$$

where $\bar{s}_{kl}$ is the associated element of $\bar{S}$. As such

$$\frac{\partial e(t)}{\partial \xi} = -k_0 cM(X_D(t) + X_N(t))M^{-1}\beta. \tag{14}$$

Dividing by $e(t)$ while multiplying by ξ_0, we produce the log-sensitivity of the error

$$\begin{aligned} s(\xi_0, t) &= \frac{\partial e(t)}{\partial \xi} \frac{\xi}{e(t)}\bigg|_{\xi=\xi_0} \\ &= \frac{\xi_0 cM(X_D(t) + X_N(t))M^{-1}\beta}{cMe^{\Lambda t}M^{-1}\beta}. \end{aligned} \tag{15}$$

Now we consider the log-sensitivity in the case of perfect tracking or when $y(t) = 1$ or $e(t) = 0$. Given a controllable

linear system where we have assigned the poles, we can guarantee convergence of $e(t)$ to zero. However, this occurs asymptotically as $t \to \infty$.

To determine whether the limit as $t \to \infty$ exists or if it diverges, we examine the ratio of the numerator and denominator of the scalar value $s(\xi_0, t)$. To simplify notation, let $cM = [z_1 z_2 \dots z_N] \in \mathbb{C}^{1\times N}$ where $z_k = \langle c, v_k \rangle$, the inner product of the row vector c with the k-th eigenvector of A. Likewise, describing the rows of M^{-1} by v_k^{-T}, we simplify the notation for the product $M^{-1}\beta$ as the column vector $w \in \mathbb{C}^{N\times 1}$ with components $\langle v_k^{-T}, \beta \rangle$.

With this, our expression for the log-sensitivity simplifies to a sum of scalars in the numerator and denominator so that

$$|s(\xi_0, t)| = \left| \frac{\partial e(t)}{\partial \xi} \frac{\xi}{e(t)} \right|_{\xi=\xi_0} = \left| \frac{\mathcal{N}(t)}{\mathcal{D}(t)} \right|, \tag{16}$$

where we have

$$\mathcal{N}(t) = \xi_0 \left(\sum_{k=1}^{N} t z_k w_k \bar{s}_{kk} e^{\lambda_k t} + \sum_{\substack{k,l=1,\\ k\neq l}}^{N} \frac{z_k w_l \bar{s}_{kl}}{\lambda_k - \lambda_l} (e^{\lambda_k t} - e^{\lambda_l t}) \right), \tag{17a}$$

$$\mathcal{D}(t) = \sum_{k=1}^{N} z_k w_k e^{\lambda_k t}. \tag{17b}$$

From this expression, we state

Theorem 1: If the dominant eigenvalue of $A = A_0 - bk + S\xi_0$ is real, the log-sensitivity $s(\xi_0, t)$ diverges linearly as $\xi_0 \bar{s}_{11} t$ as $t \to \infty$; precisely, $s(\xi_0, t) = (\xi_0(f_0 t + g_0 + \mathcal{N}_r(t)))/(h_0 + \mathcal{D}_r(t))$, where $\mathcal{N}_r(t), \mathcal{D}_r(t) \to 0$ as $t \to \infty$ and f_0, g_0, h_0 are constants.

Proof: To begin, recall that all eigenvalues have negative real part, stabilizing the system. Now, order the eigenvalues and associated eigenvectors in increasing order of the magnitude of their real parts so λ_1 is the dominant pole (i.e., it will have the dominant effect on the system as the other terms go to zero). Factoring $e^{\lambda_1 t}$ from both $\mathcal{N}(t)$ and $\mathcal{D}(t)$, we get

$$\frac{\mathcal{N}(t)}{e^{\lambda_1 t}} = \xi_0 \left(z_1 w_1 \bar{s}_{11} t + \sum_{k=2}^{N} z_k w_k \bar{s}_{kk} e^{(\lambda_k - \lambda_1)t} + \sum_{\substack{m,n=1,\\ m\neq n}}^{N} \frac{z_m w_n \bar{s}_{mn}}{\lambda_m - \lambda_n} (e^{(\lambda_m - \lambda_1)t} - e^{(\lambda_n - \lambda_1)t}) \right). \tag{18}$$

Considering the $2(N-1)$ terms of the form $e^{(\lambda_m - \lambda_1)t} - 1$ in $\mathcal{N}(t)$ that arise from this factoring of the dominant pole, this reduces to

$$\frac{\mathcal{N}(t)}{e^{\lambda_1 t}} = \xi_0 \left(z_1 w_1 \bar{s}_{11} t + \sum_{p=2}^{N} \frac{z_1 w_p \bar{s}_{1p}}{\lambda_1 - \lambda_p} - \sum_{q=2}^{N} \frac{z_q w_1 \bar{s}_{q1}}{\lambda_q - \lambda_1} + \mathcal{N}_r(t) \right) \tag{19}$$

with

$$\mathcal{N}_r(t) = \sum_{k=2}^{N} z_k w_k \bar{s}_{kk} e^{(\lambda_k - \lambda_1)t} + \sum_{\substack{m,n=2,\\ m\neq n}}^{N} \frac{z_m w_n \bar{s}_{mn}}{\lambda_m - \lambda_n} \left(e^{(\lambda_m - \lambda_1)t} - e^{(\lambda_n - \lambda_1)t} \right) - \sum_{p=2}^{N} \frac{z_1 w_p \bar{s}_{1p}}{\lambda_1 - \lambda_p} e^{(\lambda_p - \lambda_1)t} + \sum_{q=2}^{N} \frac{z_q w_1 \bar{s}_{q1}}{\lambda_q - \lambda_1} e^{(\lambda_q - \lambda_1)t} \tag{20}$$

being the terms in $\mathcal{N}(t)$ that decay to zero as $t \to \infty$.

For the denominator $\frac{\mathcal{D}(t)}{e^{\lambda_1 t}}$ we have

$$\frac{\mathcal{D}(t)}{e^{\lambda_1 t}} = z_1 w_1 + \sum_{l=2}^{2} z_l w_l e^{(\lambda_l - \lambda_1)t} = z_1 w_1 + \mathcal{D}_r(t), \tag{21}$$

where $\mathcal{D}_r(t)$ likewise decays to zero.

Now for some $T > 0$ we have that $|\mathcal{N}_r(t)| < N_0$ and $|\mathcal{D}_r(t)| < D_0$ where N_0 and D_0 are bounds at which the ratio of N_0 and D_0 to $z_1 w_1$ is negligible.

Finally, we have

$$\begin{aligned} s(\xi_0, t) &= \frac{\xi_0}{z_1 w_1 + \mathcal{D}_r(t)} \left(w_1 z_1 \bar{s}_{11} t + \sum_{p=2}^{N} \frac{z_1 w_p \bar{s}_{1p}}{\lambda_1 - \lambda_p} - \sum_{q=2}^{N} \frac{z_p w_1 \bar{s}_{q1}}{\lambda_q - \lambda_1} + N_r \right) \\ &= \xi_0 \bar{s}_{11} t + R(t), \end{aligned} \tag{22}$$

where

$$R(t) = \frac{\xi_0}{z_1 w_1 + \mathcal{D}_r(t)} \left(\sum_{p=2}^{N} \frac{z_1 w_p \bar{s}_{1p}}{\lambda_1 - \lambda_p} + \sum_{q=2}^{N} \frac{z_p w_1 \bar{s}_{q1}}{\lambda_q - \lambda_1} + \mathcal{N}_r(t) - \mathcal{D}_r(t) \bar{s}_{11} \right). \tag{23}$$

Since $\lim_{t\to\infty} R(t)$ is finite, $\xi_0 \bar{s}_{11} t$ is the dominant term of $s(\xi_0, t)$ as $t \to \infty$. ∎

Before moving to the complex-conjugate case, we note that if A has n repeated eigenvalues λ_k, with geometric multiplicity equal to n, then A is still diagonalizable. In that case, a modification to (17a) yields

$$\mathcal{N}(t) = \xi_0 \left(\sum_{k=1}^{N} t z_k w_k \bar{s}_{kk} e^{\lambda_k t} + \sum_{\substack{l\neq k\\ \lambda_k = \lambda_l}} t z_k w_l \bar{s}_{kl} e^{\lambda_k t} + \sum_{\substack{l\neq k\\ \lambda_l \neq \lambda_k}} \frac{z_k w_l \bar{s}_{kl}}{\lambda_k - \lambda_l} \left(e^{\lambda_k t} - e^{\lambda_l t} \right) \right). \tag{24}$$

If the dominant eigenvalue λ_1 is repeated n times, then one

can show that (22) is modified as

$$s(\xi_0,t)=\frac{\xi_0\left(\sum\limits_{k=1}^{n}z_kw_k\bar{s}_{kk}+\sum\limits_{\substack{p,q=1\\p\neq q}}^{n}z_pw_q\bar{s}_{pq}\right)t}{\sum\limits_{m=1}^{n}z_mw_m}+R(t), \tag{25}$$

where $R(t)$ again remains finite. Thus $s(\xi_0,t)$ again diverges linearly as $t\to\infty$ with slope given by a linear combination of the coefficients associated with the dominant, repeated eigenvalue and ξ_0.

Next we look at the case of damped, complex conjugate eigenvalues.

Theorem 2: If the dominant eigenvalue of $A=A_0-bk+S\xi_0$ appears in a complex conjugate pair $-\sigma\pm j\omega$, $\sigma>0$, then $s(\xi_0,t)=(tf(t)+g(t)+\mathcal{N}_r(t))/(h(t)+\mathcal{D}_r(t))$ where $f(t)$, $g(t)$, $h(t)$ are periodic functions with period π/ω and $\mathcal{N}_r(t)$, $\mathcal{D}_r(t)\to 0$ as $t\to\infty$ with rate given by $(\Re(\lambda_3)+\sigma)$. Thus, $s(\xi_0,t)$ has no limit as $t\to\infty$, periodically taking divergingly large local maxima and local minima.

Proof: We follow the same procedure as the proof for Theorem 1. We denote the dominant complex eigenvalue pair as $\lambda_{1,2}=-\sigma\mp j\omega$. Upon factoring the real part of the dominant pole-pair, we arrive at

$$\begin{aligned}\frac{\mathcal{N}(t)}{\xi_0e^{-\sigma t}}&=tz_1w_1\bar{s}_{11}e^{-j\omega t}+tz_2w_2\bar{s}_{22}e^{j\omega t}\\&\quad+\sum_{k=3}^{N}tz_kw_k\bar{s}_{kk}e^{(\lambda_k+\sigma)t}\\&\quad+\sum_{\substack{m,n=1,\\m\neq n}}^{N}\frac{z_mw_n\bar{s}_{mn}}{\lambda_m-\lambda_n}(e^{(\lambda_m+\sigma)t}-e^{(\lambda_n+\sigma)t}).\end{aligned} \tag{26}$$

The last term in (26) generates $2N-4$ terms of the form

$$\frac{z_{(1,2)}w_n\bar{s}_{(1,2),n}}{\lambda_{(1,2)}-\lambda_n}(e^{\mp j\omega t}-e^{(\lambda_n+\sigma)t}) \tag{27}$$

and $2N-4$ terms of the form

$$\frac{z_mw_{(1,2)}\bar{s}_{m,(1,2)}}{\lambda_m-\lambda_{(1,2)}}(e^{(\lambda_m+\sigma)t}-e^{\mp j\omega t}) \tag{28}$$

along with the pair

$$\frac{z_1w_2\bar{s}_{12}}{\lambda_1-\lambda_2}(e^{-j\omega t}-e^{j\omega t}),\quad \frac{z_2w_1\bar{s}_{21}}{\lambda_2-\lambda_1}(e^{j\omega t}-e^{-j\omega t}). \tag{29}$$

Recalling that $|\sigma|<|\Re(\lambda_l)|$, $\forall\ell\neq 1,2$, we rewrite the last term of (26) as

$$\begin{aligned}&\sum_{\substack{m,n=1,\\m\neq n}}^{N}\frac{z_mw_n\bar{s}_{mn}}{\lambda_m-\lambda_n}\left(e^{(\lambda_m+\sigma)t}-e^{(\lambda_n+\sigma)t}\right)\\&=\frac{z_1w_2\bar{s}_{12}}{\lambda_1-\lambda_2}(e^{-j\omega t}-e^{j\omega t})+\frac{z_2w_1\bar{s}_{21}}{\lambda_2-\lambda_1}(e^{j\omega t}-e^{-j\omega t})\\&\quad+\sum_{k=3}^{N}\frac{z_1w_k\bar{s}_{1k}}{\lambda_1-\lambda_k}e^{-j\omega t}+\sum_{l=3}^{N}\frac{z_2w_l\bar{s}_{2l}}{\lambda_2-\lambda_l}e^{j\omega t}\\&\quad+\sum_{m=3}^{N}\frac{z_mw_1\bar{s}_{m1}}{\lambda_m-\lambda_1}(-e^{-j\omega t})\\&\quad+\sum_{n=3}^{N}\frac{z_nw_2\bar{s}_{n2}}{\lambda_n-\lambda_2}(-e^{j\omega t})+\mathcal{N}_r(t),\end{aligned} \tag{30}$$

where $\mathcal{N}_r(t)$ contains all terms that decay to zero as $t\to\infty$. Specifically,

$$\begin{aligned}\mathcal{N}_r(t)&=\sum_{k=3}^{N}tz_kw_k\bar{s}_{kk}e^{(\sigma+\lambda_k)t}\\&\quad+\sum_{l=3}^{N}-\frac{z_1w_l\bar{s}_{1l}}{\lambda_1-\lambda_l}e^{(\sigma+\lambda_l)t}+\sum_{m=3}^{N}\frac{z_mw_1\bar{s}_{m1}}{\lambda_m-\lambda_1}e^{(\sigma+\lambda_m)t}\\&\quad+\sum_{n=3}^{N}-\frac{z_2w_n\bar{s}_{2n}}{\lambda_2-\lambda_n}e^{(\sigma+\lambda_n)t}+\sum_{p=3}^{N}\frac{z_pw_2\bar{s}_{p2}}{\lambda_p-\lambda_2}e^{(\sigma+\lambda_p)t}\\&\quad+\sum_{\substack{q,r=3,\\q\neq r}}^{N}\frac{z_qw_r\bar{s}_{qr}}{\lambda_q-\lambda_r}\left(e^{(\sigma+\lambda_q)t}-e^{(\sigma+\lambda_r)t}\right).\end{aligned} \tag{31}$$

Recalling that the eigenvalues are ordered in decreasing value of $\Re(\lambda_k)$, we note that the dominant term in $\mathcal{N}_r(t)$ goes to zero as $e^{(\lambda_3+\sigma)t}$.

Regrouping terms that do not decay to zero, we get

$$\begin{aligned}&tz_1w_1\bar{s}_{11}e^{-j\omega t}+tz_2w_2\bar{s}_{22}e^{j\omega t}+\frac{z_1w_2\bar{s}_{12}}{\lambda_1-\lambda_2}(e^{-j\omega t}-e^{j\omega t})\\&\quad+\frac{z_2w_1\bar{s}_{21}}{\lambda_2-\lambda_1}(e^{j\omega t}-e^{-j\omega t})+\sum_{k=3}^{N}\frac{z_1w_k\bar{s}_{1k}}{\lambda_1-\lambda_k}e^{-j\omega t}\\&\quad+\sum_{l=3}^{N}\frac{z_2w_l\bar{s}_{2l}}{\lambda_2-\lambda_l}e^{j\omega t}+\sum_{m=3}^{N}\frac{z_mw_1\bar{s}_{m1}}{\lambda_m-\lambda_1}(-e^{-j\omega t})\\&\quad+\sum_{n=3}^{N}\frac{z_nw_2\bar{s}_{n2}}{\lambda_n-\lambda_2}(-e^{j\omega t})\\&=tz_1w_1\bar{s}_{11}e^{-j\omega t}+tz_2w_2\bar{s}_{22}e^{j\omega t}\\&\quad+\left(\frac{z_1w_2\bar{s}_{12}}{\lambda_1-\lambda_2}-\frac{z_2w_1\bar{s}_{21}}{\lambda_2-\lambda_1}+\sum_{k=3}^{N}\frac{z_1w_k\bar{s}_{1k}}{\lambda_1-\lambda_k}\right.\\&\quad\left.-\sum_{m=3}^{N}\frac{z_mw_1\bar{s}_{m1}}{\lambda_m-\lambda_1}\right)e^{-j\omega t}+\left(-\frac{z_1w_2\bar{s}_{12}}{\lambda_1-\lambda_2}+\frac{z_2w_1\bar{s}_{21}}{\lambda_2-\lambda_1}\right.\\&\quad\left.+\sum_{l=3}^{N}\frac{z_2w_l\bar{s}_{2l}}{\lambda_2-\lambda_l}-\sum_{n=3}^{N}\frac{z_nw_2\bar{s}_{n2}}{\lambda_n-\lambda_2}\right)e^{j\omega t}\\&=tz_1w_1\bar{s}_{11}e^{-j\omega t}+tz_2w_2\bar{s}_{22}e^{j\omega t}+Qe^{-j\omega t}+Re^{j\omega t}\\&=:tf(t)+g(t).\end{aligned} \tag{32}$$

In the denominator, following the factoring of $e^{\sigma t}$, we have

$$\begin{aligned}\frac{\mathcal{D}(t)}{e^{-\sigma t}} &= z_1 w_1 e^{-j\omega t} + z_2 w_2 e^{j\omega t} + \sum_{n=3}^{N} z_n w_n e^{(\lambda_n+\sigma)t} \\ &= z_1 w_1 e^{-j\omega t} + z_2 w_2 e^{j\omega t} + \mathcal{D}_r(t) \\ &= h(t) + D_r(t).\end{aligned} \tag{33}$$

Here, $\mathcal{D}_r(t)$ denotes the terms in denominator that go to zero exponentially with dominant term $e^{(\lambda_3+\sigma)t}$. Note that for $N = 2$, the denominator is given exactly by the expression in (33) with $\mathcal{D}_r(t) = 0$.

To bound $|\mathcal{D}(t)/e^{-\sigma t}|$ we note that $|\mathcal{D}_r(t)|$ achieves its maximum for $t \in [0, \pi/\omega)$. Furthermore, the complex exponential terms in $h(t)$ will vary between $\pm 2|z_1 w_1|$. Thus, the maximum value the denominator can attain is $\left|(2|z_1 w_1|) + \max_{t\in[0,\pi/\omega)} \mathcal{D}_r(t)\right|$.

To analyze the behavior of the ratio of $\mathcal{N}(t)$ to $\mathcal{D}(t)$, we must examine the periodic behavior of $\mathcal{D}(t)$. Since z_k and w_l are, in general, complex, we must find where $|\mathcal{D}(t)| = 0$ or is a minimum. This yields the following condition for $|\mathcal{D}(t)/e^{-\sigma t}|$ as an asymptotic minimum:

$$\begin{aligned}|z_1 w_1|^2 + |z_2 w_2|^2 + 2\Re(z_1 w_1 z_2^* w_2^*)\cos(2\omega t) \\ - 2\Im(z_1 w_1 z_2^* w_2^*)\sin(2\omega t) = 0.\end{aligned} \tag{34}$$

Recalling that v_1 and v_2 (the eigenvectors associated with the dominant complex pole pair) are complex conjugates, we have $z_1 = z_2^*$ and $w_1 = w_2^*$. Combining the trigonometric functions to a single cosine term yields the equivalent, simplified, condition for the minimum of $\mathcal{D}(t)$:

$$\cos(2\omega t - \phi_{01}) = -1, \tag{35}$$

where

$$\phi_{01} := \begin{cases} \phi, & \Re(z_1 w_1 z_2^* w_2^*) > 0, \\ \phi + \pi, & \Re(z_1 w_1 z_2^* w_2^*) < 0, \end{cases} \tag{36}$$

and

$$\phi := \arctan\left(\frac{-\Im(z_1 w_1 z_2^* w_2^*)}{\Re(z_1 w_1 z_2^* w_2^*)}\right) \tag{37}$$

with arctan *defined* to be in the first or fourth quadrant. We, thus, expect the denominator to approach zero cyclically with a period $T = \pi/\omega$.

Thus, $|\mathcal{D}(t)|$ remains bounded from above, but approaches zero periodically, which produces "spikes" in the log-sensitivity characterized by

$$|s(\xi_0, t_n)| = \left|\frac{N(t_n)}{D(t_n)}\right| = \left|\frac{t_n f(t_n) + g(t_n) + \mathcal{N}_r(t_n)}{h(t_n) + \mathcal{D}_r(t_n)}\right|, \tag{38}$$

where $t_n = t_0 + n\pi/\omega$ and t_0 is the first time at which $\mathcal{D}(t)$ achieves a local minimum. In the case of $N = 2$, this is given exactly by $t_0 = (\pi + \phi_{01})/(2\omega)$. ■

IV. Classical Example – Spring-Mass System

We first examine the case of an undamped spring-mass system we wish to position at $x_{final} = 1\,\mathrm{m}$ based on an actuating force acting on the mass that provides the step-input. Taking the spring as the uncertain variable with nominal value of $k = \xi_0 = 4\,\mathrm{N/m}^2$, the state-equation for the nominal system is:

$$\begin{bmatrix}\dot{x_1} \\ \dot{x_2}\end{bmatrix} = \begin{bmatrix}0 & 1 \\ -\xi & 0\end{bmatrix}\begin{bmatrix}x_1 \\ x_2\end{bmatrix} + \begin{bmatrix}0 \\ 1\end{bmatrix} u, \tag{39}$$

where x_1 is the mass position and x_2 the velocity. We choose x_1 as the measured output so that $c = \begin{bmatrix}1 & 0\end{bmatrix}$.

Variations about the nominal value of the spring constant enter the dynamics additively though the structure matrix as $(\Delta\xi)S$ where $S = \begin{bmatrix}0 & 0 \\ 1 & 0\end{bmatrix}$.

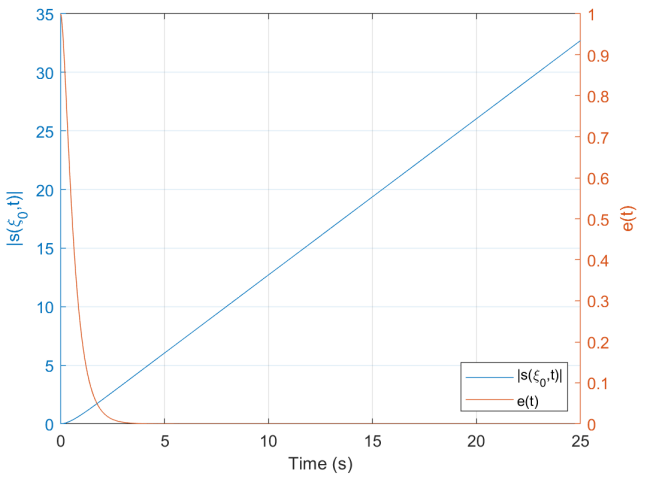

Fig. 1. Spring-mass system with $\boldsymbol{\lambda_1 = -2}$, $\boldsymbol{\lambda_2 = -5}$, $\boldsymbol{\xi_0 = 4}$, and $\boldsymbol{\bar{s}_{11} = -1/3}$. Note the linear divergence of $\boldsymbol{|s(\xi_0, t)|}$ with a slope of $\boldsymbol{4/3}$.

A. Real Eigenvalues

We first choose real, distinct eigenvalues to allow for rapid convergence with no oscillation. Choosing $\lambda_1 = -2$ and $\lambda_2 = -5$ produces a step response with zero overshoot, rise time of $1.23\,\mathrm{s}$, and settling time of $2.21\,\mathrm{s}$. The resulting limiting behavior of $|s(\xi_0, t)|$ is shown in Fig. 1. As anticipated, the log-sensitivity diverges linearly with a slope given by $|\xi_0 \bar{s}_{11}| = 4/3$.

B. Complex Eigenvalues

We now choose eigenvalues of $-1 \pm j\pi/5$ to yield a system with lighter damping and oscillatory dynamics. This provides a more gentle response with an overshoot of 0.67, rise time of $2.24\,\mathrm{s}$, and settling time of $3.52\,\mathrm{s}$. Regarding the log-sensitivity of the error, we first note that $\Re(z_1 w_1 z_2^* w_2^*) = -0.197$ and $\Im(z_1 w_1 z_2^* w_2^*) = -0.409$. Not considering the additional factor of π in ϕ_{01} produces an erroneous first zero crossing time of $t_0 = 1.61\,\mathrm{s}$. Taking into account the sign of $\Re(z_1 w_1 z_2^* w_2^*)$ agrees with the expected periodic behavior. Specifically, the system parameters yield $t_0 = (\pi + \phi_{01})/(2\omega) = 4.107\,\mathrm{s}$ and expected, asymptotic recurrence times of $t_n = t_0 + (\pi/\omega)\, n$. The results are shown in Fig. 2. We also note that the local maxima for $|s(\xi_0, t)|$ and local minima for $e(t)$ correspond to the predicated values of t_n. Finally, while showing the trend of the expected results, we note that Fig. 2 is limited

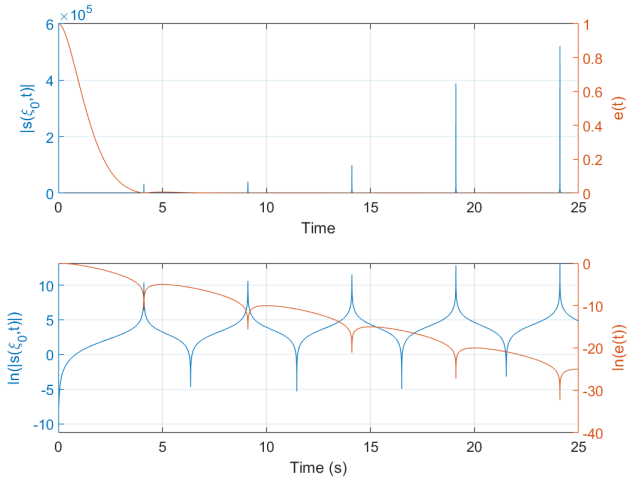

Fig. 2. Divergence of $|s(\xi_0, t)|$ for the spring-mass system with a complex eigenvalue pair at $s = -1 \pm j\pi/5$. The top plot shows both, $e(t)$ and $|s(\xi_0, t)|$, on a linear scale, and the bottom plot shows both on a log-scale. Note that $s(\xi_0, t)$ displays local maxima every $\pi/\omega = 5\,\mathrm{s}$ as the error periodically goes to zero.

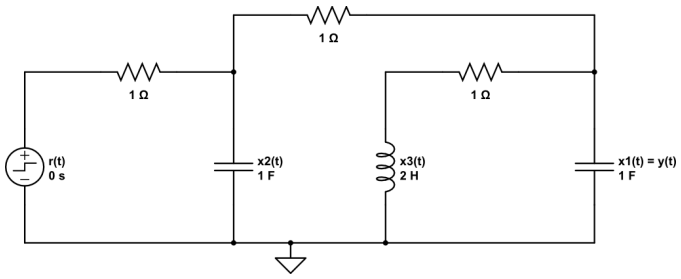

Fig. 3. RLC Circuit with three states consisting of the two capacitor voltages and single inductor current. The input is a voltage step at $t = 0$ and the output is the capacitor voltage $x_1(t)$ in the rightmost branch.

by the numerical resolution of the simulation. For $N = 2$, the analytical value of $|D(t_n)| = 0, \forall n$, while $|N(t_n)| \neq 0$, implying that $|s(\xi_0, t)|$ diverges at these times.

V. Classical Example – RLC Circuit

Extending the procedure from Section IV to a slightly more complex scenario, we consider an RLC circuit with a single inductor, two capacitors, and a voltage source input as depicted in Fig. 3.

The voltage source provides a step input of 1 V. The control objective is tracking this step input voltage at the capacitor voltage in the rightmost branch. The inductance in the system is the uncertain parameter with a nominal value of 2 H. This provides the following state-space set-up

$$\begin{bmatrix} \dot{x_1} \\ \dot{x_2} \\ \dot{x_3} \end{bmatrix} = \begin{bmatrix} -1 & 1 & -1 \\ 1 & -2 & 0 \\ \xi & 0 & -\xi \end{bmatrix} \begin{bmatrix} x_1 \\ x_2 \\ x_3 \end{bmatrix} + \begin{bmatrix} 0 \\ 1 \\ 0 \end{bmatrix} u. \tag{40}$$

$\xi_0 = 1/2$ and we have

$$S = \begin{bmatrix} 0 & 0 & 0 \\ 0 & 0 & 0 \\ 1 & 0 & -1 \end{bmatrix}. \tag{41}$$

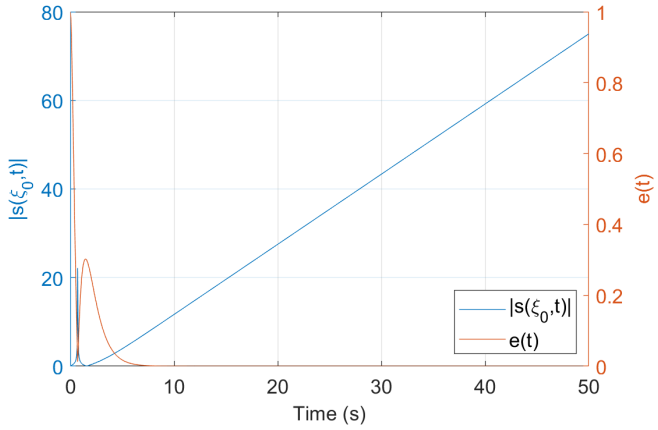

Fig. 4. Divergence of $|s(\xi_0, t)|$ for the third order circuit with $\lambda_1 = -1$, $\lambda_2 = -2$, and $\lambda_3 = -4$. As predicted, the log-sensitivity of the error diverges linearly with time.

The current through the inductor is taken as x_3 and the voltage across the output capacitor is x_1. Since we measure x_1 as the output, the output vector is $c = \begin{bmatrix} 1 & 0 & 0 \end{bmatrix}$.

A. Real Eigenvalues

We first look at a system with real eigenvalues and a dominant eigenvalue of $\lambda_1 = -1$. The system response has a rapid rise time of $0.49\,\mathrm{s}$ and a large overshoot of 30%. The behavior of the log-sensitivity with time is shown in Fig 4. As expected, we see the log-sensitivity diverge with slope $|\xi_0 \bar{s}_{11}| = |0.5(-3.167)| = 1.58$. Contrasted with this long-term behavior, we note a local maximum of $|s(t, \xi_o)|$ at $t = 0.701\,\mathrm{s}$ when the step response passes through $y(t) = 1$, attributable to the transient dynamics.

B. Complex Eigenvalues

Next, we choose complex eigenvalues of $\lambda_{1,2} = -2 \pm j\pi/10$. As seen in Fig. 5, $|s(\xi_0, t)|$ does not approach a limiting value as $t \to \infty$ but grows unbounded with periodic local maxima at a period of $\pi/\omega = 10\,\mathrm{s}$. In addition, we note a first spike in $|s(\xi_0, t)|$ at $t = 0.350\,\mathrm{s}$ when $y(t)$ passes through 1 during the transient response. The next local maximum occurs at the predicted time of $t_0 = (\pi + \phi_{01})/(2\omega) = 10.49\,\mathrm{s}$. The subsequent local maxima in $|s(\xi_0, t)|$ follow at the expected times of $t_n = (t_0 + (\pi/\omega)n) = (10.49 + 10n)\mathrm{s}$.

VI. Quantum Example – Two Qubits in a Cavity

A. System Description and Problem Formulation

We now proceed to examine how the postulated long-term behavior of the log-sensitivity applies to non-classical systems. As a first step, we examine a simple quantum system with a global steady state that any initial state will approach asymptotically, as detailed in [19]. This asymptomatic convergence provides for close similarity to the behavior of classical systems.

The system we consider consists of two qubits (quantum mechanical two-level systems) collectively coupled to one

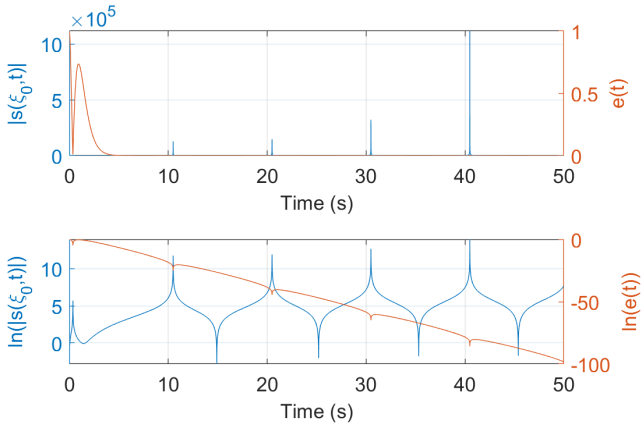

Fig. 5. $|s(\xi_0, t)|$ diverging over time for a third-order circuit with dominant complex eigenvalue pair $\lambda_{1,2} = -2 \pm j\pi/10$. The top panel displays $|s(\xi_0, t)|$ and $e(t)$ on a linear scale, and the lower panel displays the same on a log-scale. Note the periodic maxima of $|s(\xi_0, t)|$ and corresponding minima of $e(t)$ with period 10 s.

another via a lossy cavity, as originally detailed in [20]. As a quantum system, the dynamics are governed by the time-dependent Liouville equation

$$\begin{aligned}\frac{d}{dt}\rho(t) &= [H, \rho(t)] + \mathcal{L}(V_\gamma)\rho(t) \\ &= H\rho(t) - \rho(t)H + \mathcal{L}(V_\gamma)\rho(t),\end{aligned} \tag{42}$$

where the cavity has been adiabatically eliminated [20], H is the Hamiltonian that determines the evolution of the system, V_γ a constant dissipation operator, and $\rho(t)$ the density operator that encodes the state information. For this specific two-level system, we have [19]

$$H = \begin{bmatrix} 0 & \alpha_2 & \alpha_1 & 0 \\ \alpha_2^* & \Delta_2 & 0 & \alpha_1 \\ \alpha_1^* & 0 & \Delta_1 & \alpha_2 \\ 0 & \alpha_1^* & \alpha_2^* & \Delta_1 + \Delta_2 \end{bmatrix}, \tag{43a}$$

$$V_\gamma = \begin{bmatrix} 0 & \gamma_2 & \gamma_1 & 0 \\ 0 & 0 & 0 & \gamma_1 \\ 0 & 0 & 0 & \gamma_2 \\ 0 & 0 & 0 & 0 \end{bmatrix}, \tag{43b}$$

$$\rho = \begin{bmatrix} \rho_{11}(t) & \rho_{12}(t) & \rho_{13}(t) & \rho_{14}(t) \\ \rho_{12}(t)^* & \rho_{22}(t) & \rho_{23}(t) & \rho_{24}(t) \\ \rho_{13}(t)^* & \rho_{23}(t)^* & \rho_{33}(t) & \rho_{34}(t) \\ \rho_{14}(t)^* & \rho_{24}(t)^* & \rho_{34}(t)^* & \rho_{44}(t) \end{bmatrix}. \tag{43c}$$

The terms α_1 and α_2 represent the driving fields of the qubits, and Δ_1 and Δ_2 represent the detuning parameters, i.e., the difference between the driving field frequency and the qubit resonance frequency for qubits 1 and 2, respectively. The terms γ_1 and γ_2 in the matrix V_γ provide the strength of the decoherence acting on the first and second qubit respectively. We take the nominal values of α_k and γ_k terms as 1, Δ_1 as -0.1, and Δ_2 as 0.1.

We consider the following perturbations to these parameters in accordance with [19] and the associated structure matrices where δ_{mn} denotes a 4×4 matrix with a one in the m, n location and zeros elsewhere:

- Perturbation to α_1 with $S_1 = \delta_{13} + \delta_{31} + \delta_{24} + \delta_{42}$,
- Perturbations to α_2 with $S_2 = \delta_{12} + \delta_{21} + \delta_{34} + \delta_{43}$,
- Perturbations to Δ_1 with $S_3 = \delta_{33} + \delta_{44}$,
- Perturbations to Δ_2 with $S_4 = \delta_{22} + \delta_{44}$,
- Collective perturbations to γ_1 and γ_2 simultaneously with $S_5 = \delta_{12} + \delta_{13} + \delta_{24} + \delta_{34}$,
- Perturbations to γ_1 only with $S_6 = \delta_{13} + \delta_{24}$,
- Perturbations to γ_2 only with $S_7 = \delta_{12} + \delta_{34}$.

Note that the collective perturbations to the decoherence rates are mediated by the cavity, and this is what differentiates this system from a system of two independent qubits. The equations of motion do not readily lend themselves to analysis in terms of a usual state-space formalism, but we can use the Bloch formulation to accomplish this. Specifically, choosing an orthonormal basis of 4×4 Hermitian matrices σ_k, we define

$$A_{kl} = \mathrm{Tr}(jH[\sigma_k, \sigma_l]), \tag{44a}$$

$$L_{kl} = \mathrm{Tr}(V_\gamma^\dagger \sigma_k V_\gamma \sigma_l - \frac{1}{2} V_\gamma^\dagger V_\gamma \{\sigma_k, \sigma_l\}), \tag{44b}$$

$$r_k(t) = \mathrm{Tr}(\sigma_k \rho(t)). \tag{44c}$$

This produces the Bloch representation $\dot{r}(t) = (A + L)r(t)$ with $A, L \in \mathbb{R}^{16\times16}$ and $r(t) \in \mathbb{R}^{16}$. Together, with $r_0 = r(0)$, we have the standard equations that represent an autonomous state-space system with *zero-input response* $r(t) = e^{t(A+L)}r_o$.

The system has a single zero eigenvalue, and the nullspace of $A + L$ provides the steady-state associated with this zero eigenvalue, denoted as r_{ss}. We define the output as the scalar $y(t) = r_{\mathrm{ss}}^T r(t)$ where $0 \le y(t) \le 1$ and $y(t)$ represents the overlap of the current state with the steady-state. We define the overlap error as $1 - y(t) = 1 - r_{\mathrm{ss}} r(t) = cr(t)$ where $c \in R^{16\times1}$ consisting of $c_k = r_{\mathrm{ss}_k}$ for $k = 1, \ldots, 15$ and $c_{16} = \frac{3}{2}$.

To address the perturbations, S_1 through S_4 map linearly to the Bloch formulation [21], [22], [23], [24] via (44a) to produce a structure matrix $\tilde{S} \in \mathbb{R}^{16\times16}$. Thus, a differential perturbation of the form $\Delta\xi S_k$ for $k \in \{1, 2, 3, 4\}$ in (42) maps to $\Delta\xi\tilde{S}$, and we have the following perturbed form of the time evolution of the overlap error:

$$e(t) = ce^{t(A+L+\Delta\xi\tilde{S})}r_0. \tag{45}$$

This allows us to compute the derivative of $e(t)$ with respect to perturbations in ξ structured as $\tilde{S}$ in accordance with (10) and (15). Perturbations to γ_1 or γ_2 do not map linearly to the Bloch formulation and will not be considered further.

Before proceeding to the behavior of $s(\xi_0, t)$ we note:

1) In contrast to the two classical examples discussed above, there is no full-state feedback that modifies the dynamics of the system. The control is accomplished through the driving fields α_k and detuning Δ_k to modify the evolution of the state in an *a priori* manner.
2) As opposed to the classical case studies, we do not assume a zero initial state. The probability that the two-qubit ensemble is in *some* state at $t = 0$ requires a non-zero ρ_0 or equivalently $r_0 \neq 0$.

Despite these differences, the mathematical form of $e(t)$ is identical to the classical formulation and amenable to the same process for calculation of $s(\xi_0, t)$.

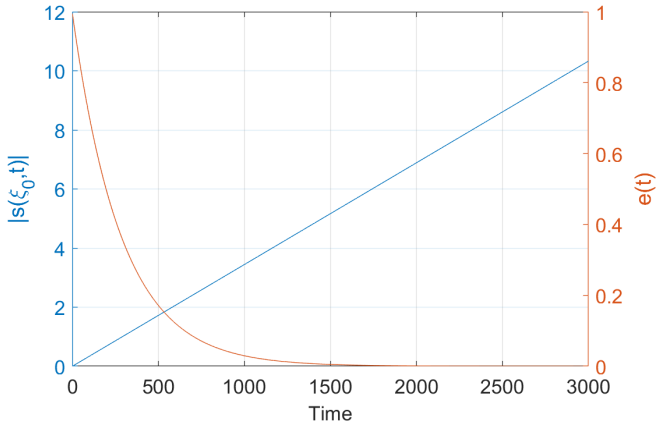

Fig. 6. Two-qubit system demonstrating linear divergence of $|s(\boldsymbol{\xi_0}, t)|$ as $r(t)$ asymptotically approaches r_{ss}. Note that the slope agrees with the predicted value of $|\boldsymbol{\xi_0 \bar{s}_{22}}| = |(1)(0.00344)| = 0.00344$.

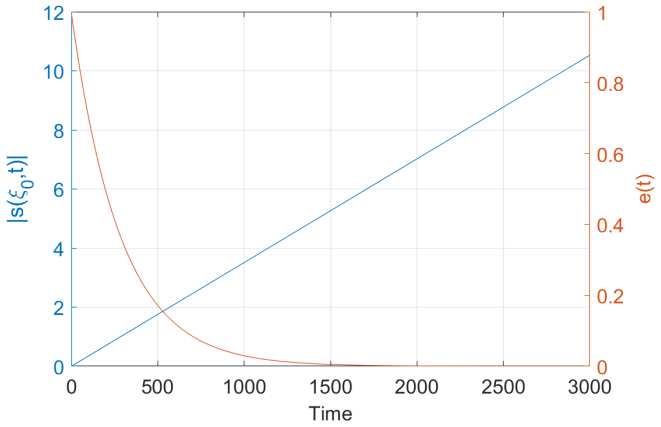

Fig. 7. Divergence of $|s(\boldsymbol{\xi_0}, t)|$ for perturbations to the detuning parameters $\boldsymbol{\Delta_{1,2}}$ with slope given by $|\boldsymbol{\bar{s}_{22}\xi_0}| = |(-0.1)(-0.0351)| = 0.00351$.

B. Log-Sensitivity of the Error

In accordance with (15), we calculate the derivative of the error to perturbations in α and Δ by

$$\begin{aligned}\frac{\partial e(t)}{\partial \xi} &= \lim_{\Delta_\xi \to 0} \frac{1}{\Delta \xi} c(e^{t(L+A+\Delta\xi\tilde{S})} - e^{t(A+L)}) r_0 \\ &= D_{\tilde{S}}(t, A+L).\end{aligned} \tag{46}$$

The two dominant eigenvalues of $A+L$ are $\lambda_1 = 0$ followed by a purely real eigenvalue of $\lambda_2 = -0.0035$. The $\bar{s}_{11}$ term is zero for all perturbations considered and does not contribute to the sum for $s(\xi_0, t)$. We thus anticipate that the behavior of $s(\xi_0, t)$ is dominated by λ_2 and the associated structure term $\bar{s}_{22}$. We expect the slope of the divergence to agree with $|\xi_0 \bar{s}_{22}|$.

The result for a differential perturbation in the driving fields α_1 or α_2 is illustrated in Fig. 6. With a nominal value of $\alpha_1 = \xi_0 = 1$ and $\bar{s}_{22} = 0.00344$, we expect a slope of 0.00344 which is borne out by Fig 6. A perturbation to α_2 with structure S_2 yields the same result.

The case for a perturbation to the detuning parameters is illustrated in Fig. 7. As anticipated, we see a slope of the divergence that agrees with $|\xi_0 \bar{s}_{22}| = |(\pm 0.1)(0.0351)| = 0.00351$.

VII. Quantum Example – Perfect State Transfer

A. System Description and Problem Formulation

We finally consider a system designed to facilitate perfect state transfer in a chain of N particles characterized by spin [25], [26]. Though the procedure can be used to facilitate state transfer for quantum states defined by multiple individual particle excited states, for simplicity, we restrict our attention to the case of transfer of a single excitation without dissipation. This is the so-called *single excitation subspace*.

As demonstrated in [25], we represent the state of the system as a column vector $\psi \in \mathbb{C}^N$ with a one in the k-th entry to denote a single excitation is associated with the k-th spin. The design goal is to produce a system that transfers the single excitation from spin 1 ($\psi_{\text{IN}} = \begin{bmatrix}1 & 0 & 0 & \cdots & 0\end{bmatrix}^T$) to N ($\psi_{\text{OUT}} = \begin{bmatrix}0 & 0 & \cdots & 1\end{bmatrix}^T$) in a finite time interval given by $T = \pi/\lambda$. Here, λ is a parameter chosen by the designer to regulate the speed of the transfer. By engineering the nearest-neighbor couplings in accordance with $J_n = \lambda/2\sqrt{n(N-n)}$ where J_n is the coupling between spins n and $n+1$, we create a Hamiltonian with J_k in the $(k, k+1)$ and $(k+1, k)$ positions for $k = 1, 2, \ldots, N-1$ and zero otherwise.

The dynamics governing the system are then given by the autonomous system

$$\dot{\psi}(t) = -jH\psi(t), \quad \psi(0) = \psi_{\text{IN}} \tag{47}$$

with solution

$$\psi(t) = e^{-jtH}\psi_{\text{IN}}. \tag{48}$$

Noting that $\psi(t)$ is complex and that the resulting overlap $f(t) = \psi_{\text{OUT}}^T \psi(t)$ is as well, we transform this to the Bloch formulation to retain congruence with the previous sections and ensure the overlap and complementary error are real values.

In this case we use the generalized Gell-Mann basis [27] of traceless, Hermitian $N^2 \times N^2$ matrices plus $1/\sqrt{2}I_{N^2}$. Applying (44a) and (44c) to the system of (47) we recast the system as

$$\dot{r}(t) = Ar(t), \; r_{\text{IN}} = r(0), \tag{49a}$$
$$r(t) = e^{tA} r_{\text{IN}}, \tag{49b}$$
$$y(t) = r_{\text{OUT}}^T r(t), \tag{49c}$$
$$e(t) = cr(t). \tag{49d}$$

r_{IN} is the Bloch-transformed version of $\rho_{\text{IN}} = |\psi_{\text{IN}}\rangle\langle\psi_{\text{IN}}|$, r_{OUT} is the transformed version of $\rho_{\text{OUT}} = |\psi_{\text{OUT}}\rangle\langle\psi_{\text{OUT}}|$, c produces the error from the current state in the same manner as Section VI and A is the Bloch-transformed Hamiltonian.

B. Log-Sensitivity of the Error

With the purely coherent dynamics given by (48) and equivalently (49), perturbations map linearly via (44a) to the Bloch formulation. For an N-chain we consider the $N-1$ possible perturbations given a change in the coupling strengths. These

are structured as S_k, an $N \times N$ matrix with zeros everywhere save for ones in the $(k+1,k)$ and $(k,k+1)$ positions. This is then mapped to an $N^2 \times N^2$ matrix in the Bloch formulation via (44a) with S interchanged with jH.

In the Bloch formulation, the matrix A has N eigenvalues at zero and the remaining $N^2 - N$ eigenvalues in purely imaginary complex conjugate pairs. As such, we do not expect $s(\xi_0, t)$ to diverge linearly. Rather, in accordance with Theorem 2, we expect the log-sensitivity to exhibit oscillations of increasing magnitude that achieve local maxima as $e(t) \to 0$ periodically as the present system is engineered to show periodicity; more general chains would show aperiodicity [28].

Note that for $N \geq 3$, the A matrix has repeated eigenvalues, requiring a modification of $s(\xi_0, t)$ as per (25). Given that A is a normal matrix, we decompose it as $A = V\Lambda V^\dagger$ where $VV^\dagger = I$. Retaining the same notation as in Section III, we have $z_k = \langle c, v_k \rangle$ and $w_l = \langle v_l^\dagger, r_0 \rangle$ where v_k is the k-th column of V and $v_l^\dagger$ is the conjugate transpose of the l-th column of V. We then compute $s(\xi_0, t)$ in accordance with (25).

In Figs. 8 and 9 we show the behavior of a two-chain with $\lambda = \pi/5$ and perturbation on the coupling between the two spins with nominal value $J_1 = \pi/10$. Fig. 10 depicts the same for a chain of three spins and perturbation on the 2–3 coupling with nominal value $J_2 = \sqrt{2}\pi/10$. In both cases, $s(\xi_0, t)$ does not have a defined limit, demonstrates the periodic spikes at times of perfect state transfer, and grows with time.

Despite the finite values for $|s(\xi_0, t)|$ in Figs. 8 and 9, it is straightforward to show that in the $N = 2$ case $|s(\xi_0, t)| = |(\pi/20)t \tan(\pi/10t)|$. This implies that the log-sensitivity diverges every $5(2n+1)$ units of time.

Additionally, we note that there is no contradiction with the assertion in earlier work [7], that under the conditions for perfect state transfer (superoptimality) the *sensitivity* of the error (equally fidelity) goes to zero. Though, [7] states this characteristic holds for rings, we can see that it also holds for the chains engineered for perfect state transfer considered here. In fact, for the $N = 2$ chain, the sensitivity has a simple form $\partial e(t)/\partial \xi = t \sin(\pi/5t)$. Thus, $\partial e(t)/\partial \xi = 0$ when $t = t_n = 5(2n+1)$. However, since $e(t) = 1/2 + 1/2\cos(\pi/5t)$, we have

$$\lim_{t \to t_n} \frac{\partial e(t)}{\partial \xi} \frac{\xi}{e(t)}\bigg|_{\xi_0} = \frac{0}{0}. \tag{50}$$

Application of L'Hopital's rule to this indeterminate form yields

$$\lim_{t \to t_n} \frac{\frac{\pi}{10}\left(\sin(\frac{\pi}{5}t) + \frac{\pi}{5}t\cos(\frac{\pi}{5}t)\right)}{-\frac{\pi}{10}\sin(\frac{\pi}{5}t)} = \frac{\pi(2n+1)}{0}, \tag{51}$$

which is consistent with the expected result for the log-sensitivity. A similar argument holds for the case of $N = 3$ with perturbation on the 2–3 coupling. For this scenario,

$$\frac{\partial e(t)}{\partial \xi} = -\frac{\sqrt{2}}{4}t\sin\left(\frac{\pi}{5}t\right) + \frac{\sqrt{2}}{8}t\sin\left(\frac{2\pi}{5}t\right), \tag{52a}$$

$$e(t) = \frac{5}{8} + \frac{1}{2}\cos\left(\frac{\pi}{5}t\right) - \frac{1}{8}\cos\left(\frac{2\pi}{5}t\right). \tag{52b}$$

TABLE I

FIDELITY VS LOG-SENSITIVITY FOR TWO- AND THREE-CHAINS AT FIRST FIDELITY MAXIMUM $t = 5$ WITH PERTURBATION OF 1–2 COUPLING.

$N = 2$, 1–2 Coupling		$N = 3$, 1–2 Coupling	
Fidelity	$\lvert s(\xi_0, t)\rvert$	Fidelity	$\lvert s(\xi_0, t)\rvert$
1.0	66664.00	1.0	24998.00
0.9999	311.95	0.9999	220.72
0.99899	97.271	0.99899	69.195
0.98999	29.264	0.98996	21.079
0.90001	7.4949	0.90008	5.6196

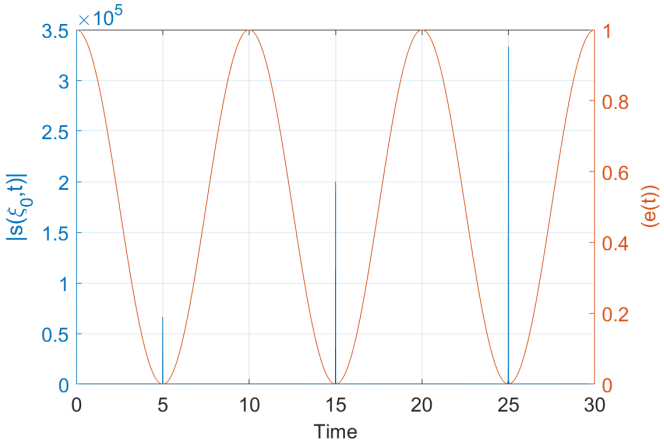

Fig. 8. Perfect state transfer for a chain of two spins with $|s(\xi_0, t)|$ and $e(t)$ plotted on a linear scale. Note that the log-sensitivity demonstrates periodic maxima at the same times as the error approaches zero.

Applying the same procedure as (50) and (51) to the equations above yields the same result: the *sensitivity* $\frac{\partial e(t)}{\partial \xi} \to 0$ as $t \to t_n$. However, the *log-sensitivity* goes to infinity at each t_n.

Furthermore, we note the trade-off between the error and the log-sensitivity – the periods of near-zero error (near perfect fidelity) correspond to those with the greatest log-sensitivity. Table I shows the trade-off between log-sensitivity and fidelity numerically.

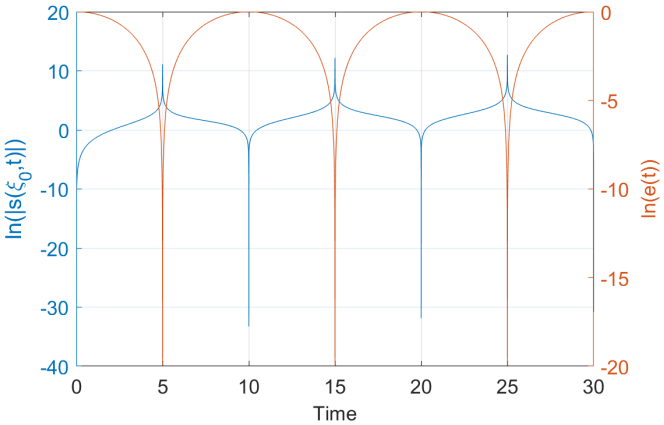

Fig. 9. Perfect state transfer for a chain of two spins with $|s(\xi_0, t)|$ and $e(t)$ plotted on a logarithmic scale.

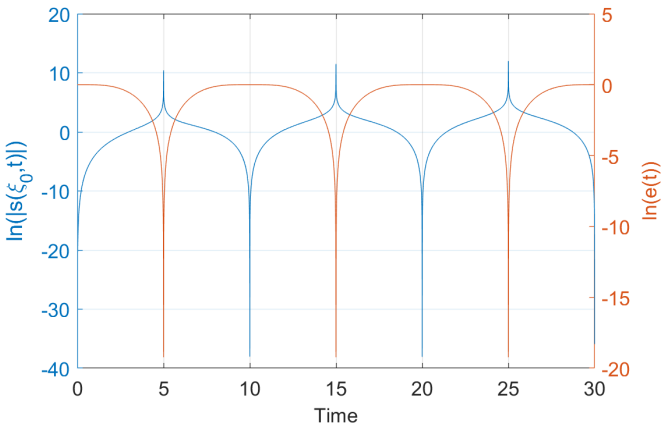

Fig. 10. Plot of $|s(\boldsymbol{\xi_0}, t)|$ and $e(t)$ on a log scale for perturbation on the J_{23} coupling.

VIII. Discussion and Conclusions

We have shown that the log-sensitivity of the error can be reliably computed from a time-domain perspective. More importantly, this robustness measure is applicable to a spectrum of classical and quantum systems and exhibits the same key characteristic: as performance increases (error gets small) the measure of performance is more sensitive to parameter variation.

Within the context of previous work on the robustness of energy landscape shaping, we can begin to see the pattern of results regarding error versus log-sensitivity unified under this time-domain specification. In [7], we demonstrate that when conditions for superoptimality prevail in a ring, the sensitivity to parameter variation vanishes. As shown in Section VII we obtain the same for chains. More importantly, while the sensitivity vanishes, the ability to analytically calculate the log-sensitivity confirms divergence at the instants of perfect state transfer, as expected when the error goes to zero. In [29], the trend of lower fidelity controllers exhibiting lower sensitivity to decoherence was observed by calculating the derivative of the error through a finite difference approximation, in agreement with the analytical methods presented here. While the overall trend suggested concordance between lower error and lower sensitivity, the trend was far from uniform. The sharp roll-off of the log-sensitivity in the range of peak fidelity seen in Table I suggest a justification for this variability of log-sensitivity for extremely high-fidelity controllers. Taken together, this suggests that designing controllers with an acceptable error and guaranteed robustness margin for a given fidelity is possible.

Finally, it is important to note that these methods work for quantum systems with and without dissipation. With some notable exceptions [17], [15], [16], previous work on the application of classical robust control techniques to quantum systems has focused on so-called *open* quantum systems (i.e., those with dissipative behaviors that lend themselves to poles that lie in the left-half plane), e.g., the mu-analysis [19] or a classically-inspired stability margin [30]. However, this work applies to *closed* quantum systems that evolve purely unitarily, without such dissipation, and lend themselves to purely imaginary eigenvalues. Given that many practical quantum systems are approximated as closed systems (although all true quantum systems are open systems), this extends the range of available classical robust control techniques, providing researchers with additional tools to explore the robustness of quantum systems. This can help to bridge the gap between classical control theory and the burgeoning field of quantum control [31], [32].

This leads to suggestions for future work. Firstly, while we have shown a classical trend between the error and log-sensitivity, we have not shown any guaranteed robustness bounds for a given error along the lines of the Bode Sensitivity Integral. A more complete theory that provides these bounds is a necessity to make this a valuable analytical tool in practice. Secondly, we have laid out a solid analytical framework for the distinct cases of real versus complex dominant eigenvalues. However, the behavior of the log-sensitivity at the transition from complex to repeated, real eigenvalues still requires attention to complete the theory. Finally, to increase applicability to quantum systems, it is necessary to extend this analysis to other, possibly non-linear, performance measures such as the fidelity error or the concurrence to measure levels of entanglement [33].

References

[1] R. Dorf, *Modern Control Systems, 13th Ed*. Pearson Prentice Hall, 2011.

[2] X. Chen, J. Zeng, H. Zhou, J. Zhao, and X. Wang, "Sensitivity analysis for time domain response of transmission lines based on the precise integration method," in *12th Int. Conf. Natural Computation, Fuzzy Systems and Knowledge Discovery, ICNC-FSKD*, pp. 1347–1351, 2016.

[3] J. Dobeš and M. Gràbner, "Using the time domain sensitivity analysis for an efficient design of symmetric microwave circuits," in *Asia-Pacific Microwave Conf., APMC*, vol. 4, pp. 4–7, 2005.

[4] B. Nouri and M. Nakhla, "Reduced-order model for time-domain sensitivity analysis of active circuits," in *22nd IEEE Workshop on Signal and Power Integrity, SPI*, pp. 1–4, 2018.

[5] L. Lombardi, M. S. Nakhla, F. Ferranti, and G. Antonini, "Time-domain sensitivity analysis of delayed partial element equivalent circuits," *Trans. Electromagnetic Compatibility*, vol. 61, pp. 1465–1473, 2019.

[6] F. C. Langbein, S. G. Schirmer, and E. Jonckheere, "Time optimal information transfer in spintronic networks," in *54th IEEE Conf. Decision and Control*, pp. 6454–6459, 2015.

[7] S. G. Schirmer, E. Jonckheere, and F. C. Langbein, "Design of feedback control laws for information transfer in spintronics networks," *Trans. Autom. Control*, 2018.

[8] S. J. Glaser, U. Boscain, T. Calarco, C. P. Koch, W. Köckenberger, R. Kosloff, I. Kuprov, B. Luy, S. Schirmer, T. Schulte-Herbrüggen, D. Sugny, and F. K. Wilhelm, "Training Schrödinger's cat: quantum optimal control," *Eur. Phys. J. D*, vol. 69, p. 279, 2015.

[9] K. Zhou and J. C. Doyle, *Essentials of Robust Control*. Prentice-Hall, 1998.

[10] K. Zhou, J. C. Doyle, and K. Glover, *Robust and Optimal Control*. Prentice-Hall, 1996.

[11] T. Walter, P. Kurpiers, S. Gasparinetti, P. Magnard, A. Potočnik, Y. Salathé, M. Pechal, M. Mondal, M. Oppliger, C. Eichler, and A. Wallraff, "Rapid high-fidelity single-shot dispersive readout of superconducting qubits," *Phys. Rev. Appl.*, vol. 7, p. 054020, 2017.

[12] D. Keith, M. G. House, M. B. Donnelly, T. F. Watson, B. Weber, and M. Y. Simmons, "Single-shot spin readout in semiconductors near the shot-noise sensitivity limit," *Phys. Rev. X*, vol. 9, p. 041003, 2019.

[13] M. Porrati and S. Putterman, "Prediction of short time qubit readout via measurement of the next quantum jump of a coupled damped driven harmonic oscillator," *Phys. Rev. Lett.*, vol. 125, p. 260403, 2020.

[14] C.-T. Chen, *Linear System Theory and Design, Fourth Edition*. Oxford University Press, 2013.

[15] D. Dong and I. R. Petersen, "Quantum control theory and its applications: a survey," *IET Control Theory and Application*, vol. 4, pp. 2651–2671, 2010.

[16] I. R. Petersen, *Robustness Issues in Quantum Control*, pp. 1–7. Springer, 2013.

[17] M. R. James, H. I. Nurdin, and I. R. Petersen, "H^∞ control of linear quantum stochastic systems," *Trans. Autom. Control*, vol. 53, no. 8, pp. 1787–1803, 2008.

[18] T. F. Havel and I. Najfeld, "Derivatives of the matrix exponential and their computation," *Adv. Appl. Math.*, vol. 16, pp. 321–375, 1995.

[19] S. G. Schirmer, F. C. Langbein, C. A. Weidner, and E. Jonckheere, "Robust control performance for open quantum systems," *Trans. Autom. Control*, 2022.

[20] F. Motzoi, E. Halperin, X. Wang, K. B. Whaley, and S. Schirmer, "Backaction-driven, robust, steady-state long-distance qubit entanglement over lossy channels," *Phys. Rev. A*, vol. 94, p. 032313, 2016.

[21] P. Rooney, A. M. Bloch, and C. Rangan, "Flag-based control of quantum purity for $n = 2$ systems," *Phys. Rev. A*, vol. 93, p. 063424, 2016.

[22] S. G. Schirmer and X. Wang, "Stabilizing open quantum systems by Markovian reservoir engineering," *Phys. Rev. A*, vol. 81, p. 062306, 2010.

[23] S. G. Schirmer, T. Zhang, and J. V. Leahy, "Orbits of quantum states and geometry of Bloch vectors for N-level systems," *J. Physics A*, vol. 37, p. 1389, 2004.

[24] F. F. Floether, P. de Fouquieres, and S. Schirmer, "Robust quantum gates for open systems via optimal control: Markovian versus non-Markovian dynamics," *New J. Physics*, vol. 14, pp. 1–26, 2012.

[25] M. Christandl, N. Datta, A. Ekert, and A. J. Landahl, "Perfect state transfer in quantum spin networks," *Phys. Rev. Lett.*, vol. 92, p. 187902, 2004.

[26] R. I. Nepomechie, "A Spin Chain Primer," *Int. J. Mod. Phys. B*, vol. 13, pp. 2973–2985, 1999.

[27] R. A. Bertlmann and P. Krammer, "Bloch vectors for qudits," *J. Phys. A: Mathematical and Theoretical*, 2008.

[28] P. Bocchieri and A. Loinger, "Quantum recurrence theorem," *Phys. Rev.*, vol. 107, no. 2, pp. 337–338, 1957.

[29] S. Schirmer, E. Jonckheere, S. O'Neil, and F. C. Langbein, "Robustness of energy landscape control for spin networks under decoherence; robustness of energy landscape control for spin networks under decoherence," in *IEEE Conf. on Decision and Control, CDC*, 2018.

[30] C. A. Weidner, S. G. Schirmer, F. C. Langbein, and E. A. Jonckheere, "Applying classical control techniques to quantum systems: entanglement versus stability margin and other limitations," in *IEEE Conf. Decision and Control, CDC*, 2022. in press.

[31] C. Brif, R. Chakrabarti, and H. Rabitz, "Control of quantum phenomena: past, present and future," *New J. Physics*, vol. 12, pp. 1–68, 2010.

[32] C. P. Koch, U. Boscain, T. Calarco, G. Dirr, S. Filipp, S. J. Glaser, R. Kosloff, S. Montangero, T. Schulte-Herbrüggen, D. Sugny, and F. K. Wilhelm, "Quantum optimal control in quantum technologies. strategic report on current status, visions and goals for research in europe," *EPJ Quantum Technology*, vol. 9, no. 1, p. 19, 2022.

[33] W. Wootters, "Entanglement of formation and concurrence," *Quantum Inf. Comput.*, vol. 1, pp. 27–44, 2001.

Sean O'Neil is a Ph.D. candidate in the Ming Hsieh Department of Electrical and Computer Engineering at the University of Southern California. He received his B.S. in Electrical Engineering from Tulane University in 2001 and completed an M.S. in Electrical Engineering from the University of Southern California in 2017. From 2017 to 2020, he served as an assistant professor of electrical engineering at the United States Military Academy. His current research centers on the extension and tailoring of robust control to quantum systems.

Sophie Schirmer (Shermer) is an Associate Professor in Physics at Swansea University, UK. SS received a PhD in Mathematics from the University of Oregon in 2000, and previously held positions as Advanced Research Fellow of the Engineering & Physical Sciences Research Council at Cambridge University, Visiting Professor at Kuopio University, Finland, and at the Open University and the University of Oregon. SS's research interests include nano-science at the quantum edge and quantum engineering, especially modeling, control and characterization of quantum systems.

Frank C. Langbein received his Mathematics degree from Stuttgart University, Germany in 1998 and a Ph.D. from Cardiff University, Wales, U.K. in 2003. He is currently a senior lecturer at the School of Computer Science and Informatics, Cardiff University, where he is a member of the visual computing group. His research interests include modeling, simulation, control and machine learning applied to quantum technologies, geometric modeling and healthcare. He is a member of the IEEE and the AMS.

Carrie A. Weidner received B.S. degrees in Engineering Physics and Applied Mathematics in 2010 and a Ph.D. in physics in 2018, all from the University of Colorado Boulder. After some time as a postdoctoral researcher, then assistant professor at Aarhus University, she is a lecturer at the University of Bristol Quantum Engineering Technology Laboratories. Her current research focuses on quantum control, sensing, and simulation, especially with ultracold atoms.

Edmond A. Jonckheere received his Engineering degree from the University of Louvain, Belgium, in 1973, Dr.-Eng. in Aerospace Engineering from the Université Paul Sabatier, Toulouse, France, in 1975, and Ph.D. in Electrical Engineering from the University of Southern California in 1978. In 1973-1975, he was a Research Fellow of the European Space Agency; in 1979, he was with the Philips Research Laboratory, Brussels, Belgium, and in 1980 he joined the University of Southern California, where he is a Professor of Electrical Engineering and Mathematics and member of the Centers for Applied Mathematical Sciences and Quantum Information Science and Technology. He is a Life Fellow of the IEEE whose research interests include conventional vs quantum control, adiabatic quantum computations, wireless networking and the power grid.